Electrochimica Acta 176 (2015) 463–471

Contents lists available at ScienceDirect

Electrochimica Acta

journal homepage: www.elsevier.com/locate/electacta

Study of the influence of boundary conditions, non ideal stimulus and dynamics of sensors on the evaluation of residence time distributions

A.N. Colli*, J.M. Bisang

Programa de Electroquímica Aplicada e Ingeniería Electroquímica (PRELINE), Facultad de Ingeniería Química, Universidad Nacional del Litoral, Santiago del Estero 2829, S3000AOM Santa Fe, Argentina

ARTICLE INFO

Article history:
Received 16 May 2015
Received in revised form 17 June 2015
Accepted 3 July 2015
Available online 10 July 2015

Keywords:
Dispersion model
Electrochemical reactors
Hydrodynamic behaviour
Dynamic response
Non-ideal behaviour
Stimulus-response method

ABSTRACT

The study of the residence time distribution is usually made in order to diagnose the hydrodynamic behaviour of the equipment. This paper reports on the residence time distribution according to six combinations of the open and closed boundary conditions, which are compared in order to determine an appropriate equation to fit experimental data from the stimulus-response method. The residence time distribution under laminar flow is analysed and the mathematical modelling of the pure convection regime, zone of axial dispersion and intermediate case is discussed. The disturbances in the residence time distribution produced by a non-ideal impulse and also by the dynamic behaviour of the sensor are quantified and the errors in its evaluation are given.

1. Introduction

The design of an electrochemical reactor requires knowledge of its hydrodynamics, which can be studied by using the stimulus-response method in order to determine the residence time distribution, RTD, of the flow inside the equipment [1]. Thus, an inert tracer is injected into the vessel inlet and its concentration in the effluent stream is measured versus time. Several signals can be used as a stimulus function, but the most common one is an instantaneous impulse in concentration at the vessel inlet, mathematically described as a Dirac delta function. The shape of the response at the vessel outlet allows to determine irregularities in the flow conditions and their correction by means of geometric changes in the equipment [2]. The response function can be processed in order to obtain characteristic parameters of the model proposed to represent the hydrodynamic behaviour of the reactor.

The implementation of the stimulus-response method, data acquisition, modelling, and ways to derive the model parameters from the residence time distribution are properly summarized in [3,4].

The effect of the injection time of the stimulus on the RTD is scarcely treated in the literature. Richardson and Peacock [5] commented that the deviation of the stimulus from the ideal pulse is irrelevant in the frequent practical cases. However, in reactors operated at high volumetric flow rates or filled with turbulence promoters the space time can be small increasing the importance of the non-ideal behaviour of the stimulus on the response of the system. Westerterp et al. [3] and Levenspiel et al. [6,7] recommended that the injection time must be lower than the reactor space time as a basic criterion for an ideal stimulus. Likewise, Levenspiel and Smith [8] show that when a stimulus is not well represented by an impulse function it is necessary to measure the RTD at the inlet and at the reactor outlet subtracting both variances. But, the measurement of the RTD at the inlet can introduce high errors because the time constant of the sensor could be in the same order of magnitude as the injection time of the tracer, which demands that the response of the system must be processed taking into account the dynamic behaviour of the sensor.

The aim of this paper is to compare different boundary conditions, earlier-presented [8–12], in order to identify the best choice to fit experimental data, including turbulent and laminar flow conditions. Also, the influence of the dynamic response of sensors and the non-ideal behaviour of the stimulus on the RTD are discussed.

2. Fundamental equations of the dispersion model

The temporal behaviour of an electrochemical reactor without reaction according to the axial dispersion model is given by [13,14]

* Corresponding author.
E-mail address: ancolli@fiq.unl.edu.ar (A.N. Colli).

http://dx.doi.org/10.1016/j.electacta.2015.07.019
0013-4686/

$$\frac{\partial c(T,Y)}{\partial T} = \frac{1}{\mathrm{Pe}}\frac{\partial^2 c(T,Y)}{\partial Y^2} - \frac{\partial c(T,Y)}{\partial Y} \quad (1)$$

where

$$T = \frac{t}{\tau} \quad (2)$$

$$\tau = \frac{\varepsilon L}{u} \quad (3)$$

$$\mathrm{Pe} = \frac{uL}{\varepsilon D_L} \quad (4)$$

and

$$Y = \frac{y}{L} \quad (5)$$

being c concentration, Pe Peclet number, t time, τ space time, T dimensionless time, L electrode length, u mean superficial fluid velocity, ε porosity, D_L dispersion coefficient, y axial coordinate along the electrode length and Y normalized axial coordinate. However, the adoption of the initial and boundary conditions represent a controversial subject. To solve Eq. (1) the following initial condition is proposed

$$T = 0 \quad c(0,Y) = \mathrm{f}(Y) \quad (6)$$

and for the boundary conditions some of the more common proposals are:

(i) At the reactor inlet and $T > 0$:for an open system

$$\frac{c(T,0)}{2} - \frac{1}{\mathrm{Pe}}\frac{\partial c(T,Y)}{\partial Y}|_{Y=0} = \mathrm{g}(T) \quad (7)$$

for a closed system with dispersion at the reactor inlet

$$c(T,0) - \frac{1}{\mathrm{Pe}}\frac{\partial c(T,Y)}{\partial Y}|_{Y=0} = \mathrm{g}(T) \quad (8)$$

for a closed system without dispersion at the reactor inlet

$$c(T,0) = \mathrm{g}(T) \quad (9)$$

(ii) At the reactor outlet and $T > 0$:
for an open system

$$c(T,\infty) = 0 \quad (10)$$

and for a closed system

$$\frac{\partial c(T,Y)}{\partial Y}|_{Y=1} = 0 \quad (11)$$

The boundary condition given by Eq. (7) considers that only half of the tracer enters into the reactor because in an open system it can diffuse in both positive and negative directions due to the initial concentration gradients [15]. Consequently, a portion of the tracer diffuses on the contrary direction to the convection flow giving that its mean residence time is lower than the space time of the reactor. Likewise, Eq. (9) means that the dispersion is neglected at the reactor inlet. Eq. (10) assumes that at a long distance from the injection point the system is not disturbed retaining the initial condition given by Eq. (6); whereas Eq. (11) neglects the dispersion at the outlet.

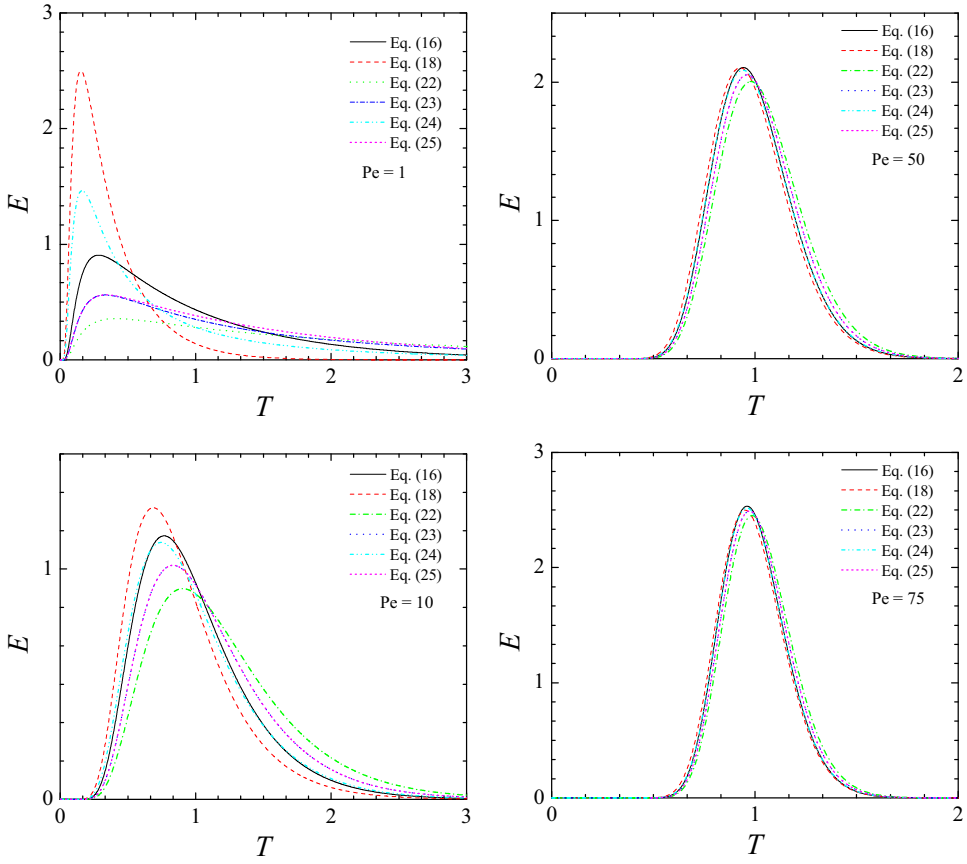

Fig. 1. Comparison of the response according to Eqs. (16),(18), (22), (23), (24) and (25) at different Peclet numbers.

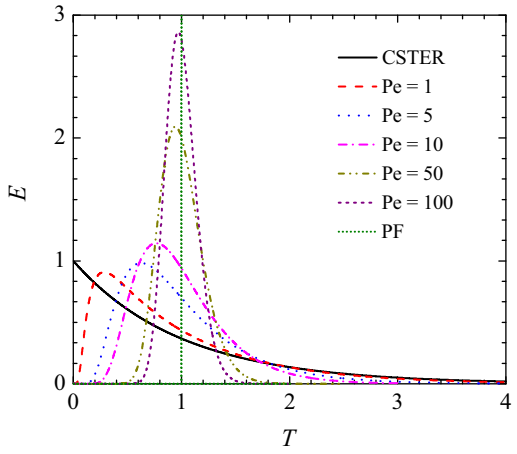

Fig. 2. Comparison of the residence time distributions of the ideal models, continuous stirred tank electrochemical reactor and plug flow, with the axial dispersion model, Eq. (16), for different values of the Peclet number.

For the study of the residence time distribution by the stimulus-response method different functions f(*Y*) and g(*T*) were proposed, being the impulse function the more frequently used according to

$$f(Y) = a\delta(Y-0) \quad \text{and} \quad g(T) = 0 \tag{12}$$

or

$$g(T) = a\delta(T-0) \text{ and } f(Y) = 0 \tag{13}$$

which will be used in the following. Here δ is the Dirac delta function and *a* is the total mass of tracer introduced in the system given by

$$a = \int_0^\infty c(T,1)\mathrm{d}T \tag{14}$$

The normalized outlet concentration, called *E* curve [1], is defined as

$$E(T) = \frac{c(T,1)}{\int_0^\infty c(T,1)\mathrm{d}T} \tag{15}$$

The solution of Eq. (1) with the boundary conditions given by Eqs. (8) and (11), called Danckwerts'boundary conditions, and Eq. (12) was reported in [9] as

$$E = 2e^{Pe/2}\sum_{n=1}^{\infty}\frac{\lambda_n^2\cos\left(\lambda_n\right)(\lambda_n^2+Pe^2/4)}{(\lambda_n^2+Pe^2/4+Pe)(\lambda_n^2-Pe^2/4)}e^{-[(Pe^2+4\lambda_n^2)/(4Pe)]T} \tag{16}$$

where λ_n are the positive roots in ascending order of the equation

$$tg(\lambda_n) = \frac{\lambda_n Pe}{\lambda_n^2 - Pe^2/4} \tag{17}$$

Furthermore, in [16,17] Eq. (1) was solved by assuming a negative step in concentration as an initial condition. In [16] Eq. (16) was

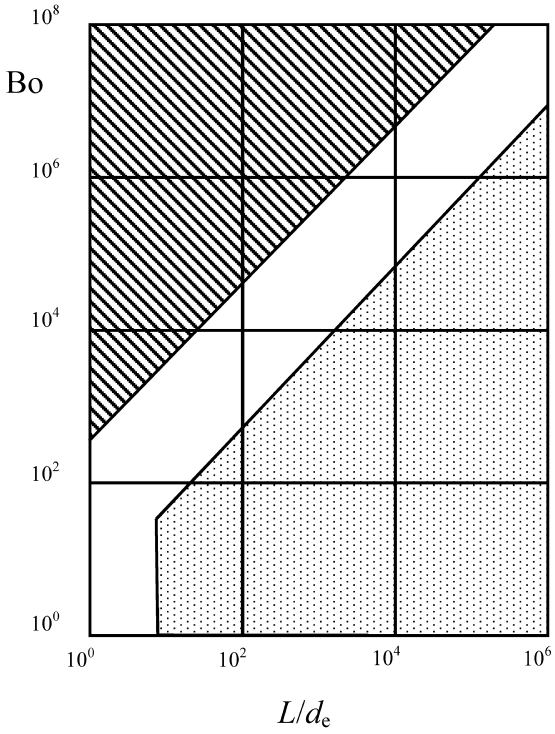

Fig. 4. Bodenstein number as a function of the aspect ratio (L/d_e). Laminar flow conditions. Dotted region: axial dispersion model. Dashed region: pure convection model. Adapted from [19].

obtained taking the first derivative of the concentration at the reactor outlet.

The numerical solution of Eq. (1), by means of an implicit finite difference method, with the boundary conditions given by Eqs. (9) and (11) and considering Eq. (12) can be written in matrix form as [10]

$$\begin{bmatrix} \beta & \gamma & 0 & 0 & 0 & 0 & 0 & 0 & 0 \\ \cdot & \cdot & \cdot & \cdot & \cdot & \cdot & \cdot & \cdot & \cdot \\ 0 & 0 & 0 & -\alpha & \beta & \gamma & 0 & 0 & 0 \\ \cdot & \cdot & \cdot & \cdot & \cdot & \cdot & \cdot & \cdot & \cdot \\ 0 & 0 & 0 & 0 & 0 & 0 & 0 & (\gamma-\alpha) & \beta \end{bmatrix} \begin{bmatrix} C(T+\Delta T,0) \\ \cdot \\ C(T+\Delta T,Y) \\ \cdot \\ C(T+\Delta T,1) \end{bmatrix} = \begin{bmatrix} C(T,0) \\ \cdot \\ C(T,Y) \\ \cdot \\ C(T,1) \end{bmatrix} \tag{18}$$

where

$$\alpha = \Delta T\left(\frac{1}{2\Delta Y} + \frac{1}{Pe\Delta Y^2}\right) \tag{19}$$

$$\beta = \left(\frac{2\Delta T}{Pe\Delta Y^2} + 1\right) \tag{20}$$

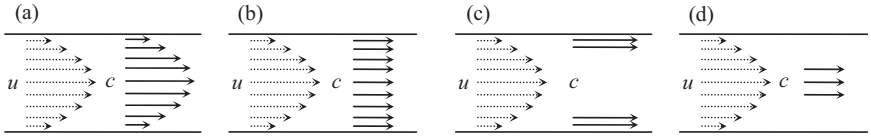

Fig. 3. Different ways to introduce the tracer. (a) injection proportional to velocity. (b) planar injection ensuring a constant concentration of tracer in the cross-section of the reactor. (c) the tracer is introduced mainly in the region of low velocities and in (d) it is only injected in the central zone.

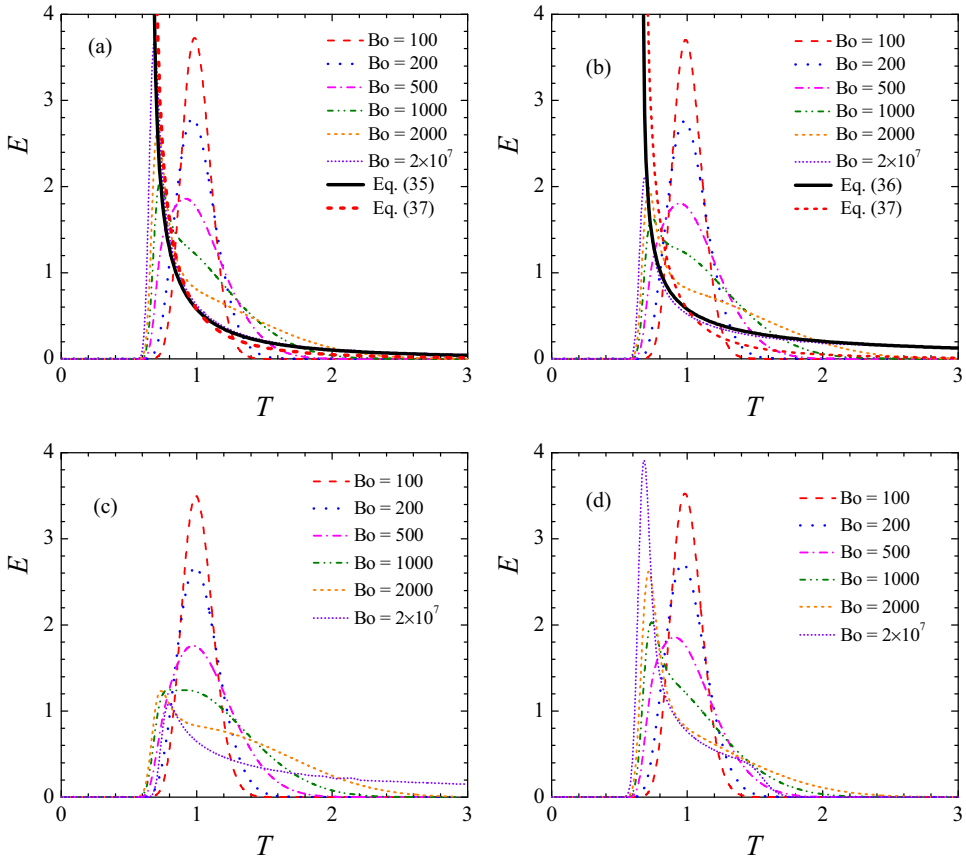

Fig. 5. Response in normalized concentration under stationary, fully developed, laminar flow from the numerical solution of Eq. (32). Each part corresponds to the way to introduce the tracer according to Fig. 3 for different values of the Bodenstein number. Full lines in Parts (a) and (b) represent the pure convection model given by Eqs. (35) and (36), respectively. Thick short dashed line: RTD according to Eq. (37). Aspect ratios: $g/W \to 0$ and $L/g = 100$.

and

$$\gamma = \Delta T\left(\frac{1}{2\Delta Y} - \frac{1}{\mathrm{Pe}\Delta Y^2}\right) \tag{21}$$

The solution of Eq. (1) for an open-open system with boundary conditions given by Eqs. (7) and (10) and Eq. (13) yields [8]

$$E = \sqrt{\frac{\mathrm{Pe}}{4\pi T}}\,\mathrm{e}^{-[\mathrm{Pe}\,(1-T)^2/4T]} \tag{22}$$

Zaisha and Jiayong [11] reported the solution of Eq. (1) as

$$E = \sqrt{\frac{\mathrm{Pe}}{\pi T}}\,\mathrm{e}^{-[\mathrm{Pe}\,(1-T)^2/4T]} - \frac{\mathrm{Pe}}{2}\mathrm{e}^{\mathrm{Pe}}\mathrm{erfc}\left(\frac{1+T}{2}\sqrt{\frac{\mathrm{Pe}}{T}}\right) \tag{23}$$

which is obtained when the boundary conditions of Eqs. (8) and (10) are taken into account together to Eq. (13).

Likewise, solving Eq. (1) for a semi-infinite dispersion system with the boundary conditions of Eqs. (9) and (10) and Eq. (13), Gibilaro [12] has obtained

$$E = \sqrt{\frac{\mathrm{Pe}}{4\pi T^3}}\mathrm{e}^{-[\mathrm{Pe}(1-T)^2/4T]} \tag{24}$$

Solving Eq. (1) with the boundary conditions of Eqs. (7) and (11) an Eq. (12) it is obtained [10]

$$E = \mathrm{e}^{\mathrm{Pe}/2}\sum_{n=1}^{\infty}\frac{\lambda_n\cos(\lambda_n)}{\left(\lambda_n + \cos(\lambda_n)\sin(\lambda_n)\right)}\mathrm{e}^{-[(\mathrm{Pe}^2+4\lambda_n^2)/(4\mathrm{Pe})]T} \tag{25}$$

where λ_n is given by

$$\mathrm{tg}(\lambda_n) = \frac{\mathrm{Pe}}{2\lambda_n} \tag{26}$$

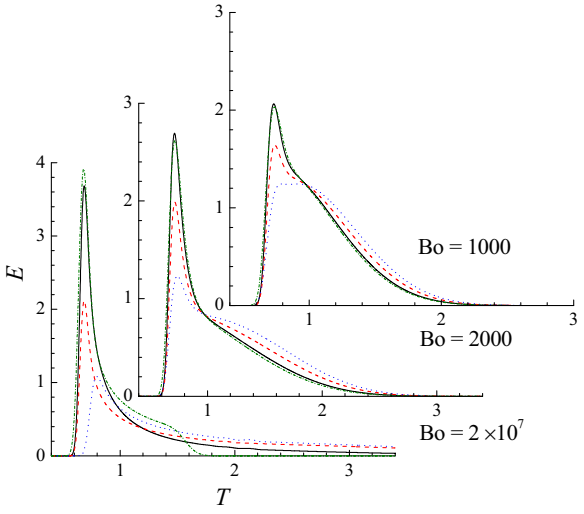

Fig. 6. Response in normalized concentration under stationary, fully developed, laminar flow from the numerical solution of Eq. (32). Each part compares the effect of the way to introduce the tracer for a given value of the Bodenstein number. The curves are in accordance to Fig. 3. (a): full line, (b): dashed line, (c): dotted line and (d): dashed-dotted line. Aspect ratios: $g/W \to 0$ and $L/g = 100$.

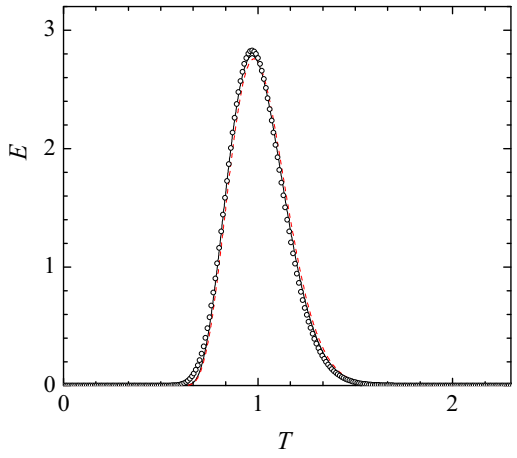

Fig.7. Comparison of residence time distributions calculated by numerical solution of Eq. (32) with the prediction according to the axial dispersion model with Danckwerts'boundary conditions given by Eq. (16). Full line: Eq. (32) with tracer injection (a), Bo = 200. Dashed line: Eq. (32) with tracer injection (b), Bo = 200. Symbols: Eq. (16) with Pe = 96.

Fig. 1 compares the temporal response of the normalized concentration according to Eqs. (16), (18), (22), (23), (24) and (25). It is observed that for low values of the Peclet number the equations show discrepancies. However, for Pe higher than 2 Eq. (23) coincides with Eq. (25) and all the calculation procedures present the same performance when the Peclet number is higher than 75. For Pe higher than 10, Eq. (24) agrees with the analytical solution of Eq. (1) with Danckwerts'boundary conditions, Eq. (16), which are frequently used for the calculation of electrochemical reactors with the dispersion model.

3. Comparison of the axial dispersion model with more simplified treatments

Applying the L'Hôspital's rule for $Pe \to 0$, the terms in the summatory of order higher than one are zero and Eq. (16) approaches

$$E(T) = e^{-T} \tag{27}$$

valid for a continuous stirred tank electrochemical reactor, CSTER.

Likewise, solving Eq. (1) for $Pe \to \infty$, with the initial and boundary conditions given by Eqs. (6) and (9), respectively, yields the temporal behaviour according to the plug flow model, PF, as

$$E(T) = \delta(T-1)H(T-1) \tag{28}$$

where the Heaviside shifting function H is defined as

$$H(T-1) = 0 \text{ for} T < 1 \tag{29}$$

$$H(T-1) = 1 \text{ for} T \geq 1 \tag{30}$$

Fig. 2. compares the temporal behaviour for different Peclet numbers according to Eq. (16), where it can observed that the predictions of Eqs. (27) and (28) represent limiting behaviours of Eq. (16). The above comparisons were based in the dispersion model with Danckwerts'boundary conditions because it was demonstrated that this model is appropriate to represent experimental results of electrochemical reactors either with low [18] or high [9] Peclet numbers.

4. Laminar flow conditions

In the case of reactors with short electrodes under laminar flow conditions each element of fluid passes its neighbour with no interaction by molecular diffusion. The residence time distribution is caused by velocity variations [19], which is called the pure convection regime, but it depends on the way to inject and to detect the tracer. Fig. 3 outlines four ways to introduce the tracer. In Part (a) the injection is proportional to velocity. Part (b) represents a planar injection ensuring a constant concentration of tracer in the cross-section of the reactor. Parts (c) and (d) show special cases. In (c), the tracer is introduced mainly in the region of low velocities and in (d) it is only injected in the central zone.

Fig. 4 reports, according to Levenspiel [19] for developed laminar flow conditions, the Bodenstein number, defined as

$$Bo = \frac{Ped_e}{L} \tag{31}$$

, as a function of the aspect ratio L/d_e, being d_e the hydraulic diameter. The Bodenstein number is used for the analysis and comparison of different electrochemical reactors with unequal length. In the dotted region is valid the axial dispersion model and in the dashed zone the pure convection regime can be used. In the intermediate region it is necessary to take into account the influence of both the velocity profile and diffusion on the residence time distribution [20]. The differential equation that describes substance spreading in laminar unidirectional flow is [21]

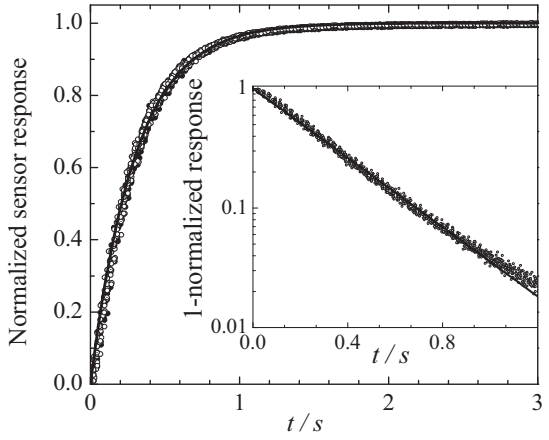

Fig. 8. Normalized transient response of the conductive cell, WTW model LTA 01, for a step change in concentration. Inset: semilogarithmic plot of the normalized transient response. Full lines: correlation of the experimental results according to Eq. (40).

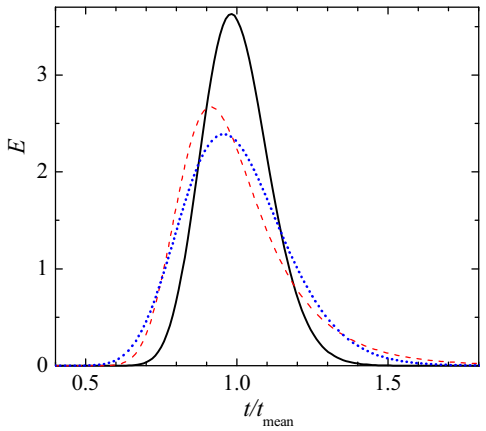

Fig. 9. Comparison of the residence time distribution considering the time constant of the sensor. Full line: $\tau_s/\tau = 0$. Dashed line: $\tau_s/\tau = 0.2$. Pe = 160. Dotted line: correlation of the dashed line with the dispersion model, Eq. (16), giving Pe = 67 as fitting parameter.

$$\frac{L\partial c}{u\partial t} = \frac{D}{uL}\left(\frac{\partial^2 c}{\partial X^2} + \frac{\partial^2 c}{\partial Y^2}\right) - \frac{u_y}{u}\frac{\partial c}{\partial Y} \tag{32}$$

being D the diffusion coefficient, u_y the velocity in the axial direction and

$$X = \frac{x}{L} \tag{33}$$

Neglecting the second derivative in the X direction and assuming a mean value for the fluid velocity along the electrode length, Eq. (32) is simplified to Eq. (1), where the deviations from the ideal behaviour are considered by means of the dispersion coefficient. To solve numerically Eq. (32), the right hand side was discretized by the method of finite volumes, giving a system of $n_x \times n_y$ ordinary differential equations that were solved with an implicit Runge-Kutta algorithm for stiff problems using a Matlab subroutine [10]. It was considered stationary, fully developed, laminar flow in a rectangular channel according to [22]

$$u_y = 12u\frac{x}{d_e}\left(1 - 2\frac{x}{d_e}\right) \tag{34}$$

The aspect ratios were $g/W \to 0$ and $L/g = 100$, being W the electrode width and g the interelectrode gap. Fig. 5 reports on the response of the calculated normalized concentration for the four ways to inject the tracer depicted in Fig. 3 and in all cases for the sampling of the tracer an average of concentration over the outlet cross section was considered. For an electrochemical reactor with infinitely wide parallel plate electrodes and fully developed laminar flow, the outlet normalized concentration in the pure convection regime is given by

$$E^*(T) = 0 \text{ for } T < \frac{2}{3} \text{ and } E^*(T) = \frac{1}{3T^2}\left(1 - \frac{2}{3T}\right)^{-1/2} \text{ for } T \geq \frac{2}{3} \tag{35}$$

when the tracer is introduced according to Fig. 3 Part (a) and

$$E^{**}(T) = 0 \text{ for } T < \frac{2}{3} \text{ and } E^{**}(T) = \frac{1}{3T}\left(1 - \frac{2}{3T}\right)^{-1/2} \text{ for } T \geq \frac{2}{3} \tag{36}$$

for the injection way given in Part (b), being $E^*(T)$ and $E^{**}(T)$ the theoretical normalized concentrations defined in [19]. The full lines in Parts (a) and (b) of Fig. (5) show the behaviour according to Eqs. (35) and (36) [19], respectively, which corroborates that the numerical solutions of Eq. (32) approaches the performance predicted by the pure convection model for high values of the Bodenstein number. Likewise, Wörner [23] generalised the residence time distributions for flow channels of different cross-sectional shape and aspect ratios, which for a rectangular channel is given by:

$$E(T) = 0 \text{ for } T < \frac{2}{3} \text{ and } E(T) = \frac{1}{3T^3}\left(1 - \frac{2}{3T}\right)^{-1/2} \text{ for } T \geq \frac{2}{3} \tag{37}$$

In Parts (a) and (b) of Fig. 5, Eq. (37) is represented as thick short dashed line showing the strong influence of the injection way on the residence time distribution.

The results of Fig. 5 are replotted in Fig. 6 in order to compare the effect of the way to inject the tracer in the reactor for different values of the Bodenstein number. Figs. 5 and 6 show that in the regions of intermediate regime and under pure convection the temporal behaviour of the reactor is strongly dependent on the way to introduce the tracer. Under laminar flow conditions, it is necessary to pay attention to the design of the experiment and the care used to conduct the tracer study.

Fig. 7 makes a comparison between the residence time distribution according to the axial dispersion model with Danckwerts'boundary conditions, Eq. (16), with the temporal behaviour obtained by numerical solution of Eq. (32) when the tracer is introduced in the ways (a) and (b) of Fig. 3. Fig. 7 corroborates that for Bodenstein numbers lower than 200 the axial dispersion model is appropriate for calculating the residence time distribution in the reactor, being also independent on the way to introduce or to detect the tracer.

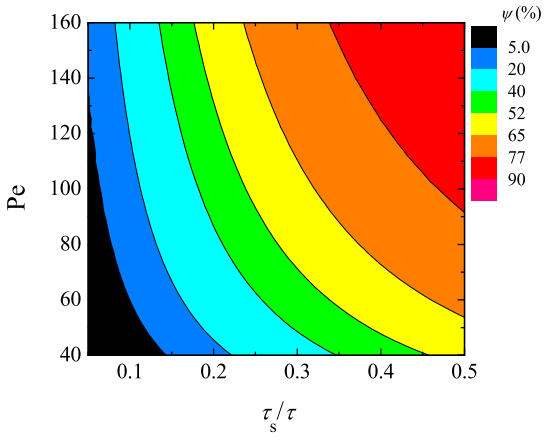

Fig. 10. Contour plot of the error between the residence time distributions considering the time constant of the sensor as a function of the Peclet number and the ratio between the time constant of the sensor and the space time of the reactor. Contour height numbers are the error values according to Eq. (43).

5. Consideration of the time constant of the sensor

For small reactors or high volumetric flow rates the space time can be of the same order of magnitude of the time constant of the sensor, which requires to modify the above equations in order to obtain accurate values of the Peclet number.

Applying Laplace transformation to Eq. (1) with the initial and boundary conditions given by Eqs. (6), (8) and (11), respectively, and Eq. (13) yields

$$c(s,1) = \frac{4a\sigma e^{Pe/2}}{(\sigma+1)^2 e^{\sigma Pe/2} - (\sigma-1)^2 e^{-\sigma Pe/2}} \tag{38}$$

where s is the Laplace transform variable and

$$\sigma = \sqrt{1 + 4s/Pe} \tag{39}$$

Fig. 8 shows the dynamic behaviour of a platinum conductivity cell formed by two parallel plate electrodes, WTW model LTA 01, with a cell constant of 0.114 cm^{-1}. To obtain Fig. 8, the conductivity cell was suddenly immersed in an electrolytic solution and its conductivity was measured as a function of time. This procedure was repeated for NaOH and KCl solutions with different concentrations. The inset in Fig. 8 shows the data plotted in a semilogarithmic scale, which are independent on the kind of electrolyte solutions and on its concentration. The linearity of the data in the inset suggests that the dynamic behaviour of the conductivity cell, as concentration sensor, can be represented by a first order system according to

$$\tau_s \frac{dc_s(t)}{dt} + c_s(t) = h(t) \tag{40}$$

being τ_s the time constant of the sensor and c_s its response in concentration for a perturbation given by $h(t)$. For the results reported on Fig. 8, $h(t)$ is a step perturbation in concentration. The slope of the line in the inset of Fig. 8 gives $\tau_s = 0.3$ s and the full lines represent the result of the correlation. Applying Laplace transformation to Eq. (40), combining with Eq. (38) and taking into account

Table 1
Experimental conditions for the tracers.

Tracer	Concentration	Conductivity range* / mS cm^{-1}	Injected volume / cm^3	Volumetric flow rate / dm^3 min^{-1}
NaOH	0.15–30 wt%	0.1–2.0	0.2–2.5	0.5–6
KCl	0.2 wt%–sat.	0.1–2.0	0.2–2.5	0.5–6

* In the detection point.

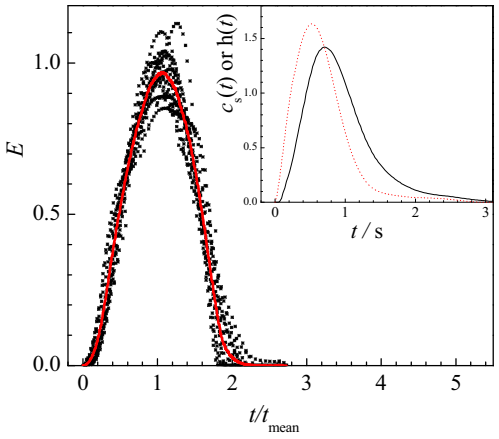

Fig. 11. Non-ideal impulse for the different tracers. Symbols: experimental points. Full line: smoothed values of the experimental results. Inset: concentration measured by the conductivity meter, full line, and its correction by the constant time of the sensor, dashed line.

Eq. (2), the residence time distribution for an ideal impulse results in

$$E(s) = \frac{4\sigma e^{Pe/2}}{\left[(\sigma+1)^2 e^{\sigma Pe/2} - (\sigma-1)^2 e^{-\sigma Pe/2}\right]\left(\frac{\tau_s}{\tau}s+1\right)} \quad (41)$$

The inversion of Eq. (41) from the complex s plane to the time plane was made by a numerical Laplace transform inversion method [24], using a Fourier series approximation with a Matlab subroutine [25]. Fig. 9 shows as full line the residence time distribution according to the dispersion model and in the dashed line was taken into account the time constant of the sensor, Eq. (41). In these calculations it was assumed Pe = 160 and $\tau_s/\tau = 0.2$, where it can be observed a strong influence of the sensor on the measurement of the dynamic behaviour. The curves in Fig. 9 are referred to the mean residence time in the reactor, t_{mean}, defined as

$$t_{mean} = \frac{\int_0^\infty t c(t) dt}{\int_0^\infty c(t) dt} \quad (42)$$

instead of τ, because the sensor shifts the distribution giving a t_{mean} value higher than τ and displacing the dashed line to the left of the full line. Likewise, the dotted line in Fig. 9 was obtained by correlation of the dashed line with the dispersion model, Eq. (16), obtaining Pe = 67 as fitting parameter. The high discrepancy between the full and dotted lines points to the need to consider the effect of the time constant of the sensor on the RTD for the correlation of experimental results in order to obtain the Peclet number. This effect is more pronounced as smaller is the space time between the injection and detection points, as in the measurement of the RTD at the reactor inlet. Fig. 10 displays a contour plot of iso-error between the residence time distributions with and without regard to the time constant of the sensor, as a function of both the Peclet number and the ratio between the time constant of the sensor and the space time of the reactor. The error in the evaluation of the residence time distributions was calculated as

$$\psi = \int_0^\infty |E^{ideal\ impulse}_{,\tau_s=0} - E^{ideal\ impulse}_{,\tau_s\neq 0}| d(t/t_{mean}) \quad (43)$$

Fig. 10 reveals that to obtain an error lower than 5 % the ratio between τ_s and τ must be lower than 0.1, the exact value depends on the Peclet number.

6. Injection time

For the experimental determination of residence time distributions by means of the stimulus-response method an impulse function is usually used as stimulus, which is frequently simulated by manually injecting, with a syringe, of a small volume of a tracer into the reactor inlet during a short time. The injection time of the tracer in order to approximate the impulse function is a controversial subject. The aim of the present section is to propose a quantitative criterion regarding to the ideal behaviour of the stimulus. Thus, a volume of tracer was injected and its concentration was measured, by conductimetry, close to the injection point. Table 1 summarizes the range of experimental conditions of the tracers and Fig. 11 shows the experimental RTD near the injection point, where it can be observed that the experimental distributions show the same shape independent of the kind and volume of tracer and also of the volumetric flow rate. These experimental data were corrected by the constant time of the sensor using Eq. (40). The inset in Fig. 11 shows as full line a typical curve of the concentration detected by the conductivity meter and as dashed line its correction taking into account the time constant of the sensor, h (t), where a strong influence of the dynamic of the sensor on the response is observed due to the small distance between the injection and detection points. Likewise, the full line in Fig. 11 corresponds to the smoothed values of the experimental results, which were used in the model as stimulus at the reactor inlet, function g(T), instead of the impulse function, Eq. (13). The theoretical residence time distribution was calculated solving numerically Eq. (1) with the initial and boundary conditions given by Eqs. (6), (8) and (11), respectively, and Eq. (13) by using the implicit finite difference method, as it was previously outlined [9]. Fig. 12 compares typical curves of the residence time distributions for the axial dispersion model using as stimulus the ideal impulse function, represented as a thick full line, with the temporal behaviour when is used a non-ideal stimulus according to Fig. 11.

It must be emphasized that when a non-ideal impulse is used as stimulus the mean residence time of the tracer, $t_{mean,tracer}$, differs from the space time because the tracer is not injected all together into the reactor. Thus, in the abscissae of Fig. 12 t/t_{mean} is again used instead of τ. Each graph in Fig. 12 corresponds to a Peclet number value and the curves at each graph depends on the parameter R_t, defined as

$$R_t = \frac{\tau}{t_{mean,\ tracer}} \quad (44)$$

As expected when R_t increases the response of the system approaches the ideal stimulus. To compare the curves reported in Fig. 12, it is convenient to define the error in the calculation of the residence time distribution as

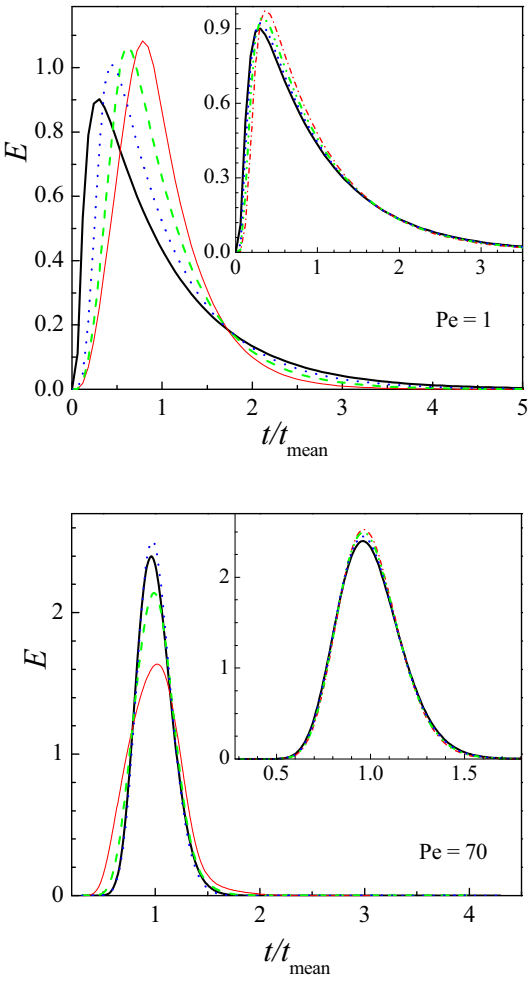

Fig. 12. Comparison of the residence time distributions for an ideal and non-ideal impulse stimulus for different values of Pe number. Thick full lines: ideal stimulus, Eq. (13). Full lines: $R_t = 1$, dashed lines: $R_t = 2$, dotted lines: $R_t = 5$. Insets: dashed dotted lines: $R_t = 10$, dashed dotted dotted lines: $R_t = 20$ and short dashed lines: $R_t = 50$.

$$\psi = \int_0^\infty |E^{\text{ideal}}_{\text{impulse}} - E^{\text{non ideal}}_{\text{impulse}}| d(t/t_{\text{mean}}) \quad (45)$$

Fig. 13 shows a contour plot of iso-error, ψ, between the residence time distributions as a function of both the Peclet number and the parameter R_t. In Fig. 13 it can be observed that errors lower than 4.8% correspond to the region on the right hand side of the dashed lines, which can be represented by the following empirical equations:

$$R_t \geq 24 - 0.16\text{Pe for } 10 < \text{Pe} < 100 \quad (46)$$

and

$$R_t \geq 38 - 2\,\text{Pe for } 0.1 < \text{Pe} < 10 \quad (47)$$

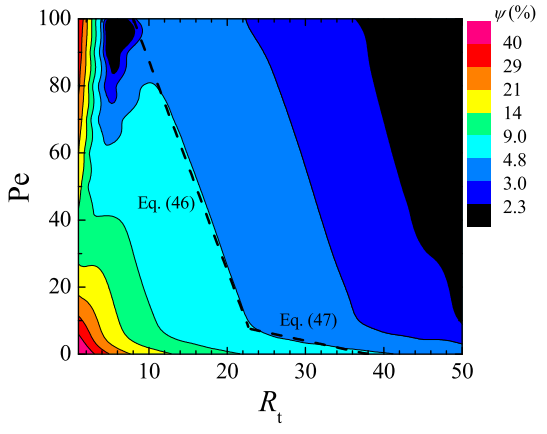

Fig. 13. Contour plot of the error between the residence time distributions for an ideal and non-ideal impulse as a function of the Peclet number and the parameter R_t. Contour height numbers are the error values according to Eq. (45).

Fig. 13 allows to estimate the injection time for a given error, as two times the value of $t_{\text{mean,tracer}}$, or alternatively the calculation with the use of Eqs. (46) or (47) yields errors lower than 4.8%.

7. Conclusions

The design of electrochemical reactors under turbulent flow conditions is frequently performed by using the axial dispersion model with Danckwerts'boundary conditions. In these cases and for Pe higher than 10, the calculation of the Peclet number by fitting of experimental data obtained with the use of the stimulus-response method can be made with Eq. (24) instead of Eq. (16), requiring less computation time.

Under laminar flow conditions it becomes necessary to identify if the system is under pure convection regime, in the zone of axial dispersion or in the intermediate case to use the appropriate algorithm to fit the temporal behaviour of the reactor. Furthermore, in pure convection regime or in the intermediate one the reproducibility of experiments is constrained by the uneven distribution of the tracer injected with a syringe.

The calculation of reliable values of Peclet number from experimental data requires knowing the dynamic behaviour of the sensor, whose time constant must be lower than 10% of the reactor space time to ensure an error in the measurement of the residence time distribution lower than 5%.

The injection time of the tracer can be estimated by using Eqs. (46) or (47) to achieve a stimulus close to the ideal impulse giving a minimal disturbance in the residence time distribution.

A mean residence time higher than the space time can be attributed to the impulse is non-ideal or to the influence of the dynamics of the sensor.

Acknowledgements

This work was supported by the Agencia Nacional de Promoción Científica y Tecnológica (ANPCyT), Consejo Nacional de Investigaciones Científicas y Técnicas (CONICET) and Universidad Nacional del Litoral (UNL) of Argentina.

References

[1] P.V. Danckwerts, Continuous flow systems. Distribution of residence times, Chemical Engineering Science 2 (1953) 1.
[2] E.R. Henquín, A.N. Colli, M.E.H. Bergmann, J.M. Bisang, Characterization of a bipolar parallel-plate electrochemical reactor for water disinfection using low conductivity drinking water, Chemical Engineering and Processing: Process Intensification 65 (2013) 45.
[3] R.K. Westerterp, W.P.M. Van Swaaij, A.A.C.M. Beenackers, Chemical Reactor Design and Operation, 2nd Ed., John Wiley & Sons, New York, 1988.
[4] S.H. Fogler, Elements of Chemical Reaction Engineering, 4th Ed., Prentice Hall, New Jersey, 2005.
[5] J.F. Richardson, D.G. Peacock, Coulson and Richardson's Chemical Engineering, 3rd Ed., Chemical and Biochemical Reactors and Process Control, Volume 3, Elsevier, Netherlands, 1994.
[6] O. Levenspiel, J.C.R. Turner, The interpretation of residence-time experiments, Chemical Engineering Science 25 (1970) 1605.
[7] O. Levenspiel, B.W. Lai, C.Y. Chatlynne, Tracer curves and the residence time distribution, Chemical Engineering Science 25 (1970) 1611.
[8] O. Levenspiel, W.K. Smith, Notes on the diffusion-type model for the longitudinal mixing of fluids in flow, Chemical Engineering Science 6 (1957) 227.

[9] A.N. Colli, J.M. Bisang, Evaluation of the hydrodynamic behaviour of turbulence promoters in parallel plate electrochemical reactors by means of the dispersion model, Electrochimica Acta 56 (2011) 7312.
[10] A.N. Colli, PhD Thesis, Universidad Nacional del Litoral, 2013, http://bibliotecavirtual.unl.edu.ar:8180/tesis/handle/1/519?locale=en
[11] M. Zaisha, C. Jiayong, On the response function and residence time distribution of the axial dispersion model for tubular reactors, Chinese Journal of Chemical Engineering 7 (1992) 173.
[12] L.G. Gibilaro, On the residence time distribution for systems with open boundaries, Chemical Engineering Science 33 (1978) 487.
[13] K. Scott, Electrochemical Reaction Engineering, Academic Press Inc., London, 1991.
[14] O. Levenspiel, Chemical Reaction Engineering, 3rd Ed., Wiley, 1998.
[15] P. Trinidad, C. Ponce de León, F.C. Walsh, The application of flow dispersion models to the FM01-LC laboratory filter-press reactor, Electrochimica Acta 52 (2006) 604.
[16] S. Yagi, T. Miyauchi, On the residence time curves of the continuous reactors, Kagaku Kogaku 17 (1953) 382.
[17] T. Otake, E. Kunugita, A. Kawabe, Mixing characteristics of irrigated packed towers, Chemical Engineering 23 (1959) 81.
[18] A.N. Colli, J.M. Bisang, Generalized study of the temporal behaviour in recirculating electrochemical reactor systems, Electrochimica Acta 58 (2011) 406.
[19] O. Levenspiel, Tracer Technology: Modeling the Flow of Fluids, Springer-Verlag, New York Inc, 2011.
[20] K. Steffani, B. Platzer, Influence of velocity profile and diffusion on residence time distributions: mesoscopic modeling and application to Poiseuille flow, Chemical Engineering and Processing: Process Intensification 41 (2002) 143.
[21] S.D. Kolev, W.E. van der Linden, Laminar dispersion in parallel plate sections of flow systems used in analytical chemistry and chemical engineering, Analytica Chimica Acta 247 (1991) 51.
[22] F.M. White, Fluid Mechanics, 4th Ed., McGraw-Hill, 2003.
[23] M. Wörner, Approximate residence time distribution of fully develop laminar flow in a straight rectangular channel, Chemical Engineering Science 65 (2010) 3499.
[24] R.G. Rice, D.D. Do, Applied Mathematics And Modeling For Chemical Engineers, 2dn Ed., Wiley-AIChE, 2012.
[25] K.J. Hollenbeck, INVLAP.M:, A matlab function for numerical inversion of Laplace transforms by the de Hoog algorithm, 1998, http://www.mathworks.com/matlabcentral/answers/uploaded_files/1034/invlap.m.